Online ISSN 1848-3380, Print ISSN 0005-1144
ATKAFF 55(4), 425–433(2014)

Changqing Qiu, Shenghua Huang, Ende Wang

Direct Active Power Control for Regenerative Cascade Inverter with Reduced AC Power in DC Link

DOI 10.7305/automatika.2014.12.545
UDK 681.537:621.314.54.072
IFAC 3.1.1; 4.6

Original scientific paper

This paper presents a regenerative cascade inverter topology with direct active power control scheme. From the mathematical model of the proposed regenerative cascade inverter, the instantaneous active power and reactive power are derived. Based on the instantaneous *abc* theory, direct active power feed-forward control is proposed to reduce AC power and voltage fluctuation in DC link. Moreover, a load current full order observer is established to avoid the inconvenient of the current sensor installation. The proposed control scheme is analyzed theoretically by simulation, and verified experimentally.

Key words: Regenerative cascade inverter, Direct active power control, Feed-forward control, Observer

Upravljanje aktivnom snagom regenerativnog kaskadnog invertera uz smanjenje izmjenične komponente snage u istosmjernom međukrugu. U ovome radu predstavljena je topologija regenerativnog kaskadnog invertera sa shemom direktnog upravljanja aktivnom snagom. Trenutna aktivna i reaktivna snaga dobiveni su iz matematičkog modela predloženog regenerativnog kaskadnog invertera. Na temelju *abc* teorije, predloženo je unaprijedno upravljanje aktivnom snagom kako bi se smanjila izmjenična komponenta snage i promjena napona u istosmjernom međukrugu. Ugradnja senzora za mjerenje struje izbjegla se razvijanjem observera punog reda. Predložena shema upravljanja testirana je simulacijski i eksperimentalno.

Ključne riječi: regenerativni kaskadni inverer, upravljanje aktivnom snagom, unaprijedno upravljanje, observer

1 INTRODUCTION

In recent years, H-bridge cascade inverters have proved to be an effective alternative to medium voltage AC drives [1,2]. The traditional H-bridge cascade topology, using diodes to obtain a DC link voltage of each power cell, is not able to permit the regeneration of power from AC motor to the grid and is not applicable to some equipment, such as downhill conveyors and traction. On the other hand, H-bridge inverter in power cell generates a second harmonic DC link voltage [3], thus, large electrolytic capacitors have to be used to reduce DC link voltage fluctuation.

To achieve regeneration, PWM rectifiers instead of diode rectifiers allow the topology to regenerate power to the grid [4,5]. The transformer leakage inductances are used as the input filter inductances. Therefore, power cell is composed of a three-phase PWM rectifier, DC link electrolytic capacitors and an H-bridge inverter, as shown in Fig. 1.

However, the important problem is that input and output instantaneous active power of power cell is unbalanced in this cascade topology, generating the second harmonic DC link voltage. The load power feed-forward control scheme [5-7], which is one of direct power control (DPC) schemes, is proposed to reduce capacitance energy storage requirements and the second harmonic voltage. Based on the instantaneous *pq* theory [8], the DPC schemes are directly controlled in *dq* synchronous reference frame [9-11]. Another important problem is the asymmetric three-phase input currents due to unbalanced equivalent leakage inductances. The current control scheme in the positive and negative sequence *dq* references is applied with a new instantaneous reactive power definition [12]. Extracting sequential components and solving a set of nonlinear equations in real-time are not easy to achieve in fixed point DSP. In [13], a proportional resonant (PR) controller in the stationary $\alpha\beta$ frame without extracting sequential components is proposed and positive and negative sequence currents can be controlled together. In the previous literatures, the current reference calculations are based on the instantaneous *pq* theory. In order to avoid complex calculations of extracting positive and negative sequence *dq* current reference, based on instantaneous *abc* theory [14], direct active

power control (DAPC) scheme in the stationary *abc* frame is developed.

The DPC scheme, which requires a current sensor to measure the DC link load current, could result in difficulties for the laminated bus bar. To implement the feed-forward control without measuring the DC link load current, DC link load current observers were proposed. In [15], disturbance observers are designed for implementing the feed-forward control for a single-phase PWM rectifier in control of the DC link voltage. In [16], an observer for disturbance estimation is introduced to compensate source voltage unbalances. However, there is no comprehensive and detailed analysis on the digital realization of observers and the design principles of gain matrix.

This paper is organized as follows. Section 2 describes mathematical model and control scheme of regenerative H-bridge cascade inverter. The analysis of DC link load current observer is discussed in Section 3. Section 4 covers the simulation results. The experimental verification is presented in Section 5. The conclusions are drawn in Section 6.

2 PROPOSED TOPOLOGY OF REGENERATIVE H-BRIDGE CASCADE INVERTER AND ITS CONTROL SCHEME

2.1 Proposed topology

Figure 1 shows the proposed topology of regenerative H-bridge cascade inverter and the equivalent circuit of its power cell. This structure uses three symmetrical power cells [as shown in Fig. 1 (b)] connected in series to form one motor phase voltage. The carrier-based modulating technique is used for the H-bridge cascade inverter [1,2]. Each power cell is combined through a magnetic interface, called a multi-winding transformer. The PWM rectifier directly connects to the secondary side of the multi-winding transformer without the bulky filter inductances. Meanwhile, phase-shifted structure does not need in the transformer secondary side.

Because the transformer secondary structure are identical and the coupling between the secondary windings is possible to ignore, while the AC grid and leakage inductance of primary side are converted to the secondary side, each power cell can be controlled independently. Carrier-based modulating technique is also used in PWM rectifier. Therefore, low switching frequency of PWM rectifier can obtain good input current waveform.

2.2 Mathematical model of H-bridge inverter and motor

Figure 1 (b) shows the equivalent topology for H-bridge inverter and induction motor in which i_d and i_q denote d_q frame stator currents, u_d and u_q denote *dq* frame stator voltages and *N* denotes H-bridge cascaded number.

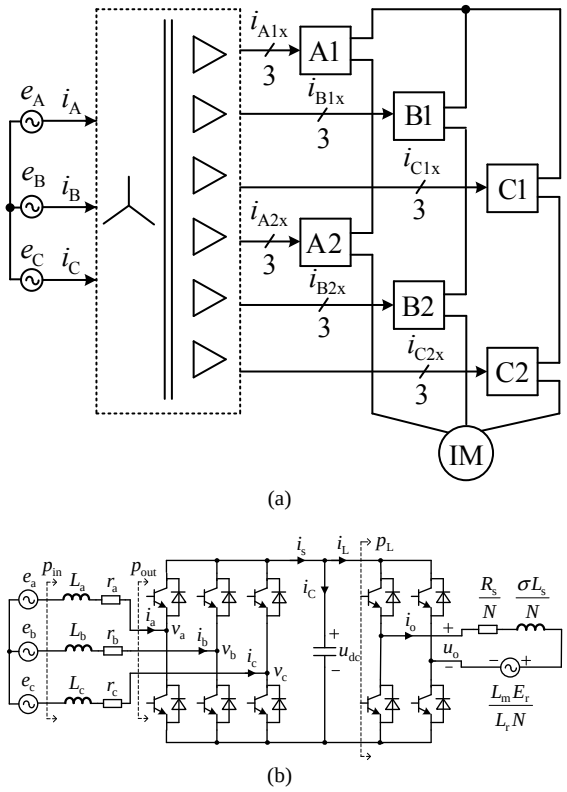

Fig. 1. Regenerative H-bridge cascade inverter: (a) overall topology (x=a, b, c), (b) equivalent circuit of power cell

In the rotor flux orientation scheme, the stator current of induction motor dynamics is given by

$$\begin{cases} \sigma L_s \frac{\mathrm{d}i_\mathrm{d}}{\mathrm{d}t} = -R_\mathrm{s} i_\mathrm{d} + \omega_\mathrm{s} \sigma L_s i_\mathrm{q} + u_\mathrm{d} \\ \sigma L_s \frac{\mathrm{d}i_\mathrm{q}}{\mathrm{d}t} = -R_\mathrm{s} i_\mathrm{q} - \omega_\mathrm{s} \sigma L_s i_\mathrm{d} + u_\mathrm{q} - \frac{\omega_\mathrm{s} L_\mathrm{m} \psi_\mathrm{r}}{L_\mathrm{r}} \end{cases}, \quad (1)$$

where L_m, L_s, L_r, R_s, ω_s, E_r, and ψ_r are the mutual inductance, stator inductance, rotor inductance, stator resistance, electrical angular frequency, rotor induced electromotive force, and d axis rotor flux, respectively.

The output fundamental voltage u_o and fundamental current i_o of the inverter is given by

$$\begin{cases} u_\mathrm{o} = \sqrt{2}(u_\mathrm{d} \cos \omega_\mathrm{s} t - u_\mathrm{q} \sin \omega_\mathrm{s} t)/(\sqrt{3}N) \\ i_\mathrm{o} = \sqrt{2}(i_\mathrm{d} \cos \omega_\mathrm{s} t - i_\mathrm{q} \sin \omega_\mathrm{s} t)/\sqrt{3} \end{cases}. \quad (2)$$

Considering the output of H-bridge inverter as an unbalanced three-phase four-wire system, and then the instantaneous current and voltage components at the motor side in the stationary $\alpha\beta 0$ frame can be obtained

$$\begin{bmatrix} i_{\mathrm{o}\alpha} \\ i_{\mathrm{o}\beta} \\ i_{\mathrm{o}0} \end{bmatrix} = \mathrm{T}_{\mathrm{abc}-\alpha\beta 0} \begin{bmatrix} i_\mathrm{o} \\ 0 \\ 0 \end{bmatrix} = \begin{bmatrix} \sqrt{2/3} i_\mathrm{o} \\ 0 \\ \sqrt{1/3} i_\mathrm{o} \end{bmatrix}, \quad (3)$$

$$\begin{bmatrix} u_{o\alpha} \\ u_{o\beta} \\ u_{o0} \end{bmatrix} = \mathrm{T}_{abc-\alpha\beta0} \begin{bmatrix} u_o \\ 0 \\ 0 \end{bmatrix} = \begin{bmatrix} \sqrt{2/3}u_o \\ 0 \\ \sqrt{1/3}u_o \end{bmatrix}, \quad (4)$$

where the Clarke's transformation matrix $\mathrm{T}_{abc-\alpha\beta0} = \sqrt{2/3}\begin{bmatrix} 1 & -1/2 & -1/2 \\ 0 & \sqrt{3}/2 & -\sqrt{3}/2 \\ 1/\sqrt{2} & 1/\sqrt{2} & 1/\sqrt{2} \end{bmatrix}$.

According to the *pq* theory in three-phase four-wire systems [8], instantaneous active and reactive power can be obtained

$$\begin{aligned} p_L &= u_{o\alpha}i_{o\alpha} + u_{o\beta}i_{o\beta} + u_{o0}i_{o0} = u_o i_o \\ &= [(u_d i_d + u_q i_q) + k\cos(2\omega_s t + \phi)\ ]/3N \end{aligned}, \quad (5)$$

where $k = \sqrt{(u_d i_d - u_q i_q)^2 + (u_d i_q + u_q i_d)^2}$,
$\phi = \arctan[(u_d i_q + u_q i_d)/(u_d i_d - u_q i_q)]$.

$$q_L = u_{o\beta}i_{o\alpha} - u_{o\alpha}i_{o\beta} = 0. \quad (6)$$

From (5), p_L contains a DC component and an oscillating component at twice the motor electrical frequency.

2.3 Mathematical model of PWM rectifier

Figure 1 (b) shows the equivalent topology for PWM rectifier of power cell in which e_a, e_b, and e_c are the grid voltage sources; L_x and r_x (x=a, b, c) stand for the equivalent filter inductance and resistance of each phase; v_a, v_b, and v_c are the input terminal voltage. After the Clarke's transformation, the dynamic model of PWM rectifier in the stationary $\alpha\beta$ frame can be expressed as

$$E_{\alpha\beta} = \bar{R}I_{\alpha\beta} + \bar{L}\frac{dI_{\alpha\beta}}{dt} + V_{\alpha\beta} + \tilde{R}\tilde{I}_{\alpha\beta} + \tilde{L}\frac{d\tilde{I}_{\alpha\beta}}{dt}, \quad (7)$$

where $\bar{R} = (r_a + r_b + r_c)/3$, $\bar{L} = (L_a + L_b + L_c)/3$,

$$\tilde{R} = (2r_a - r_b - r_c)/6 + j(r_b - r_c)/2\sqrt{3},$$

$$\tilde{L} = (2L_a - L_b - L_c)/6 + j(L_b - L_c)/2\sqrt{3}.$$

The variables $E_{\alpha\beta} = e_\alpha + je_\beta$, $V_{\alpha\beta} = v_\alpha + jv_\beta$, and $I_{\alpha\beta} = i_\alpha + ji_\beta$ are positive sequence space vectors of the grid voltage, the input terminal voltage, and the input current, respectively. $\tilde{I}_{\alpha\beta} = i_\alpha - ji_\beta$ is the complex conjugate of $I_{\alpha\beta}$. $\bar{R}$ and $\bar{L}$ are employed to describe the effect of unbalanced impedances on the positive sequence voltage. Meanwhile, $\tilde{R}$ and $\tilde{L}$ represent the effect of unbalanced impedances on the negative sequence vector.

2.4 Instantaneous active and reactive power of PWM rectifier

For maintaining a constant DC link voltage, the power fed into PWM rectifier must instantaneously balance the power drawn by the motor load in the inverter. Instantaneous active and reactive power is given a clear physical meaning and formula in the stationary $\alpha\beta$ frame [8]. Therefore, by ignoring the IGBT switch losses, control objectives of input instantaneous active and reactive power are shown in (8) as

$$\begin{cases} p_{in}(t) = p_L(t) \\ q_{in}(t) = 0 \end{cases}. \quad (8)$$

Suppose that the grid voltage vector is $E_{\alpha\beta} = Ee^{j\omega_e t}$. Under these conditions of the given (5) and (8), the reference current vector of PWM rectifier is then expressed by

$$I_{\alpha\beta} = Ie^{j\omega_e t} = (I_{con} + I_{osc}\cos(2\omega_s t + \phi))e^{j\omega_e t}, \quad (9)$$

where $I_{con} = (u_d i_d + u_q i_q)/(3NE)$,
$I_{osc} = k/(3NE)$.

From (7) and (9), the voltage vector $V_{\alpha\beta}$ must be

$$\begin{aligned} V_{\alpha\beta} &= V_p e^{j\omega_e t} + V_n e^{-j\omega_e t} \\ &= [E - (\bar{R} + j\omega_e\bar{L})I + 2\omega_s\bar{L}I_{osc}\sin(2\omega_s t + \phi)]e^{j\omega_e t} \\ &+[(j\omega_e\tilde{L} - \tilde{R})I + 2\omega_s\tilde{L}I_{osc}\sin(2\omega_s t + \phi)]e^{-j\omega_e t} \end{aligned}. \quad (10)$$

Due to unbalanced equivalent leakage inductance of the transformer, PWM rectifier should provide a positive sequence part $V_p e^{j\omega_e t}$ and a negative-sequence part $V_n e^{-j\omega_e t}$ simultaneously.

While the complex output power can be defined in the stationary $\alpha\beta$ frame as

$$S_{out} = V_{\alpha\beta}\tilde{I}_{\alpha\beta}. \quad (11)$$

Substituting (9) and (10) to (11) yields the complex power. Then, the instantaneous active power, delivered to the DC link, is obtained as

$$p_{out}(t) = Re\{S_{out}\} = p_o + p_{c2}\cos 2\omega_e t + p_{s2}\sin 2\omega_e t, \quad (12)$$

where $p_o = EI - \bar{R}I^2 + 2\omega_s\bar{L}I_{osc}I\sin(2\omega_s t + \phi)$,

$$p_{c2} = -(R_{re} + \omega_e L_{im})I^2 + 2\omega_s L_{re}I_{osc}I\sin(2\omega_s t + \phi),$$

$$p_{s2} = (-R_{im} + \omega_e L_{re})I^2 + 2\omega_s L_{im}I_{osc}I\sin(2\omega_s t + \phi).$$

It is worth noting that the instantaneous active power delivered to the DC link contains the DC average term, besides, some extra harmonics at $2\omega_e$, $2\omega_s$, $4\omega_s$, $2(\omega_e \pm \omega_s)$ and $2(\omega_e \pm 2\omega_s)$.

The definition of the instantaneous reactive power under unbalanced conditions has already been addressed. The expression of quadrature complex power using a new definition in [12] is given by

$$S'_{out} = V'_{\alpha\beta}\tilde{I}_{\alpha\beta} = (-je^{j\omega_e t}V_p + je^{-j\omega_e t}V_n)(e^{-j\omega_e t}I). \quad (13)$$

After expanding the terms and rearranging the real part of (13), the instantaneous reactive power delivered to the DC link can be expressed as

$$q_{\rm out}(t) = Re\{S'_{\rm out}\} = q_{\rm o} + q_{\rm c2}\cos 2\omega_{\rm e}t + q_{\rm s2}\sin 2\omega_{\rm e}t, \tag{14}$$

where $q_{\rm o} = -\omega_{\rm e}\bar{L}I^2$,

$$q_{\rm c2} = (R_{\rm im} - \omega_{\rm e}L_{\rm re})I^2 - 2\omega_{\rm s}L_{\rm im}I_{\rm osc}I\sin(2\omega_{\rm s}t + \phi),$$

$$q_{\rm s2} = -(R_{\rm re} + \omega_{\rm e}L_{\rm im})I^2 + 2\omega_{\rm s}L_{\rm re}I_{\rm osc}I\sin(2\omega_{\rm s}t + \phi).$$

It is worth noting from (12) and (14) that the terms of p_{c2} have the same magnitudes as those of q_{s2}, and so do the terms of p_{s2} and q_{c2}.

2.5 Proposed input active power control scheme

In order to guarantee that the active and reactive instantaneous motor powers are supplied by the PWM rectifier, the DC link voltage should be constant. Therefore, besides the load power feed-forward, additional active power is taken from the grid voltage to compensate for the overall losses of the power cell. With the active power reference p_{ref} as the voltage controller output, given by

$$p_{\rm ref} = (K_{\rm vp} + \frac{K_{\rm vi}}{s})[\frac{(u^*_{\rm dc})^2 - u^2_{\rm dc}}{2}] + p_{\rm o}, \tag{15}$$

where K_{vp} and K_{vi} are proportional gain and integral gain, respectively. Design of the PI parameters in the voltage loop is proposed in [17].

The current decoupling control scheme in *dq* synchronous reference frame requires the exact parameters of the filter inductance to extract the positive and negative sequence. However, the equivalent leakage inductance parameters of power cells are not exactly equal. Consequently, in order to eliminate the fluctuating components of the input instantaneous active power,active and non-active current calculation based on instantaneous *abc* theory are used [14]. Thus, the *abc* phase input current references by means of a minimization method can be calculated as

$$\begin{bmatrix} i^*_{\rm a} \\ i^*_{\rm b} \\ i^*_{\rm c} \end{bmatrix} = \frac{p_{\rm ref}}{e^2_{\rm a} + e^2_{\rm b} + e^2_{\rm c}} \begin{bmatrix} e_{\rm a} \\ e_{\rm b} \\ e_{\rm c} \end{bmatrix}. \tag{16}$$

The main objective of DAPC scheme using the *abc* theory is to obtain the current references with minimum root mean square (RMS) value, capable of delivering the active power of the motor.

The current loop is implemented in the stationary *abc* frame. As the current references are sinusoidal, proportional plus resonant (PR) controllers are adopted to reach fast dynamic response and zero tracking error in steady state. Furthermore, the PR controllers can remove the effect of the grid disturbance. In order to eliminate the regulating errors for multiple frequency currents, such as ($\omega_e \pm 2\omega_s$), the PR controller is expressed as

$$\begin{aligned} D({\rm s}) = {} & K_{\rm ip} + \frac{K_{\rm ir}s}{s^2+\omega_{\rm c}s+\omega^2_{\rm e}} \\ & + \frac{K_{\rm ir}s}{s^2+\omega_{\rm c}s+(\omega_{\rm e}+2\omega_{\rm s})^2} + \frac{K_{\rm ir}s}{s^2+\omega_{\rm c}s+(\omega_{\rm e}-2\omega_{\rm s})^2} \end{aligned}, \tag{17}$$

where K_{ip}, K_{ir}, and ω_c are proportional gain, resonant gain, and the 3 dB bandwidth, respectively. Coefficient ω_c=(0~15) rad/s is suggested in [18,19], K_{ip} and K_{ir} are determined by [17,20].

Based on the above analysis, the schematic diagram of the proposed controller is shown in Fig. 2.

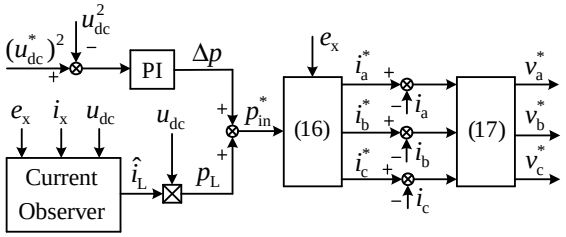

Fig. 2. The proposed control system block diagram

Unlike the traditionally schemes, the proposed input active power control scheme does not need the coordinate transformation and the extraction of sequential components. This scheme is very simple and has a strong robustness.

2.6 Ideal overall input current

Figure 1 (a) shows the topology in which the power cell A1, B1, and C1 are the same cascaded number. If the power fed into PWM rectifier instantaneously balance the power drawn by the motor in H-bridge inverter, and the IGBT switch is lossless, then $\Delta p = 0$, thus the desired AC currents i_{A1x} (x=a, b, c) at the input of the power cell A1, using (16), are given by (18)–(20) for a, b, and c phase, respectively

$$\begin{aligned} i_{\rm A1a} = {} & C_1\cos\omega_{\rm s}t + C_2\cos(\omega_{\rm s}t + 2\omega_{\rm e}t + \phi) \\ & + C_2\cos(\omega_{\rm s}t - 2\omega_{\rm e}t + \phi) \end{aligned}, \tag{18}$$

$$\begin{aligned} i_{\rm A1b} = {} & C_1\cos(\omega_{\rm s}t - 2\pi/3) + C_2\cos(\omega_{\rm s}t + 2\omega_{\rm e}t + \phi \\ & - 2\pi/3) + C_2\cos(\omega_{\rm s}t - 2\omega_{\rm e}t + \phi - 2\pi/3)] \end{aligned}, \tag{19}$$

$$\begin{aligned} i_{\rm A1c} = {} & C_1\cos(\omega_{\rm s}t + 2\pi/3) + C_2\cos(\omega_{\rm s}t + 2\omega_{\rm e}t + \phi \\ & + 2\pi/3) + C_2\cos(\omega_{\rm s}t - 2\omega_{\rm e}t + \phi + 2\pi/3)] \end{aligned}, \tag{20}$$

where $C_1 = (u_{\rm d}i_{\rm d} + u_{\rm q}i_{\rm q})/(3NE)$, $C_2 = k/(3NE)$.

Input currents, which contain harmonic at $\omega_s \pm 2\omega_e$, provide active power oscillation components for the inverter side. Similarly, the current given by (21) is a phase current in the power cell B1, and (22) is a phase current in the power cell C1, all of which feature harmonics at frequencies $\omega_s \pm 2\omega_e$, but 240 out of phase

$$\begin{aligned} i_{\mathrm{B1a}} &= C_1 \cos\omega_{\mathrm{s}} t + C_2 \cos(\omega_{\mathrm{s}} t + 2\omega_{\mathrm{e}} t + \phi - 4\pi/3) \\ &\quad + C_2 \cos(\omega_{\mathrm{s}} t - 2\omega_{\mathrm{e}} t + \phi - 4\pi/3) \end{aligned} . \tag{21}$$

$$\begin{aligned} i_{\mathrm{C1a}} &= C_1 \cos\omega_{\mathrm{s}} t + C_2 \cos(\omega_{\mathrm{s}} t + 2\omega_{\mathrm{e}} t + \phi + 4\pi/3) \\ &\quad + C_2 \cos(\omega_{\mathrm{s}} t - 2\omega_{\mathrm{e}} t + \phi + 4\pi/3) \end{aligned} . \tag{22}$$

Therefore, these harmonics are cancelled out by the combined operation of the power cells that belong to the same cascaded number. In fact, the total contribution to a phase of the first cascaded number of power cells (A1, B1, and C1) is the summation of the currents given by (18), (21), and (22), which comes to be

$$i_{\mathrm{A}} = 3C_1 \cos\omega_{\mathrm{s}} t. \tag{23}$$

Thus, the operation of the same cascaded number of power cells guarantees the overall input grid currents with unity power factor which are due to the proposed control scheme.

3 LOAD CURRENT OBSERVER

If the active load current can be calculated, the dynamic response to load transients can be improved to satisfy the wide range load change. A reasonable method is to estimate the load current directly with the measured DC link voltage and input AC currents. In order to implement the design results into practical digital control systems, the design is directly carried out in discrete domain. The discrete domain observer as shown below

$$\begin{cases} \begin{bmatrix} u_{\mathrm{dc}}(k+1) \\ i_{\mathrm{L}}(k+1) \end{bmatrix} = \mathrm{A} \begin{bmatrix} u_{\mathrm{dc}}(k) \\ i_{\mathrm{L}}(k) \end{bmatrix} + \mathrm{B}\,[i_{\mathrm{s}}(k)] \\ u_{\mathrm{dc}}(k) = \mathrm{C} \begin{bmatrix} u_{\mathrm{dc}}(k) \\ i_{\mathrm{L}}(k) \end{bmatrix} \end{cases}, \tag{24}$$

where DC input current $i_{\mathrm{s}}(k) = (e_{\mathrm{a}} i_{\mathrm{a}} + e_{\mathrm{b}} i_{\mathrm{b}} + e_{\mathrm{c}} i_{\mathrm{c}})/u_{\mathrm{dc}}$, sampling period T_s, state vector $x(k) = [\ u_{\mathrm{dc}}(k) \quad i_{\mathrm{L}}(k)\ ]^{\mathrm{T}}$, state matrix $\mathrm{A} = \begin{bmatrix} 1 & -\frac{T_{\mathrm{s}}}{C_{\mathrm{d}}} \\ 0 & 1 \end{bmatrix}$, input matrix $\mathrm{B} = \begin{bmatrix} \frac{T_{\mathrm{s}}}{C_{\mathrm{d}}} & 0 \end{bmatrix}^{\mathrm{T}}$, output matrix $\mathrm{C} = \begin{bmatrix} 1 & 0 \end{bmatrix}$. The block diagram of the load current observer is then drawn in Fig. 3.

Where the observer state vector $\hat{x}(k)$, according to formula (24), the next state can be predicted by

$$\overline{x}(k+1) = \mathrm{A}\widehat{x}(k) + \mathrm{B}u(k). \tag{25}$$

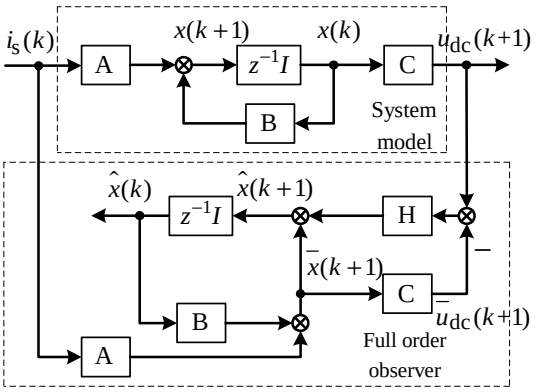

Fig. 3. The block diagram of the load current observer

The state correction vector is generated by feeding back the difference between the estimated DC link voltage and the actual output, which is expressed by:

$$\Delta\hat{x}(k+1) = \mathrm{H}[y(k+1) - \mathrm{C}\overline{x}(k+1)], \tag{26}$$

where $\mathrm{H} = [\ H_1 \quad H_2\ ]^{\mathrm{T}}$ is a gain matrix. Therefore, the dynamic equation of the observer is then written as:

$$\begin{aligned} \widehat{x}(k+1) &= \overline{x}(k+1) + \mathrm{H}[y(k+1) - \mathrm{C}\overline{x}(k+1)] \\ &= (\mathrm{A} - \mathrm{HCA})\ \widehat{x}(k) + (\mathrm{B} - \mathrm{HCB})u(k) + \mathrm{H}y(k+1) \end{aligned} . \tag{27}$$

The characteristic equation is expressed by

$$z^2 + (H_1 - \frac{T_{\mathrm{s}}}{C_{\mathrm{d}}} H_2 - 2)z + 1 - H_1 = 0. \tag{28}$$

To achieve stable solution, the poles of the observer must have all its two roots within the unit circle. Meanwhile, to allow the observer convergence rate faster than the original model, the observer poles are placed at *k* times of the original poles, where $0<k<1$. H can be solved by

$$\begin{cases} H_1 = 1 - k^2 \\ H_2 = -\frac{C_d}{T_s}(k-1)^2 \end{cases} . \tag{29}$$

The estimated DC link load current can be obtained

$$\widehat{i}_{\mathrm{L}}(k+1) = H_2 \Delta U_{\mathrm{dc}}(k) + (1 + \frac{H_2 T_{\mathrm{s}}}{C_{\mathrm{d}}})\widehat{i}_{\mathrm{L}}(k) - \frac{H_2 T_{\mathrm{s}}}{C_{\mathrm{d}}} i_{\mathrm{s}}(k), \tag{30}$$

where $\begin{cases} \widehat{U}_{\mathrm{dc}}(k) = \widehat{U}_{\mathrm{dc}}(k-1) + H_1 \Delta U_{\mathrm{dc}}(k-1) \\ \qquad + T_{\mathrm{s}}(1 - H_1)(i_{\mathrm{s}}(k-1) - \widehat{i}_{\mathrm{L}}(k-1))/C_{\mathrm{d}} \\ \Delta U_{\mathrm{dc}}(k) = U_{\mathrm{dc}}(k+1) - \widehat{U}_{\mathrm{dc}}(k) \end{cases}$.

Table 1. Parameters used in the power cell

Parameters	Value	Parameters	Value
L_a	4.6 mH	r_a	0.1 Ω
L_b	3.8 mH	r_b	0.1 Ω
L_c	3 mH	r_c	0.1 Ω
e_a	47cos($\omega_e t$) V	u_{dc}	100 V
e_b	47cos($\omega_e t$-2π/3) V	C_d	1038μF
e_c	47cos($\omega_e t$+2π/3) V	T_s	1/10000 s

4 SIMULATION RESULTS

To validate the feasibility of the proposed control scheme under unbalanced input filter inductances, both experimental and simulation tests have been carried out with the parameters given in Tab. 1. Suppose that the filter inductance parameters do not know during the experiment, only in accordance with L=3 mH and r=0.1 Ω to design the parameters of the PR controller (K_{ip}=3 V/A, K_{ir}=300 V/A·s and ω_c=5 rad/s).

The waveform of the motor current, estimated DC link load current, input current, and DC link voltage are shown in Fig. 4, when the motor synchronous speed increases from 5 Hz to 35 Hz. When 0 to 0.2 s, the motor is running in 5 Hz. After 0.2 s, the motor begins to accelerate. The motor speeds up to 35 Hz until 0.8 s. When 0.8 s to 1 s, the stable running of the motor in 35 Hz. Throughout the acceleration process, the load current is identified in real time. The fluctuation of DC link voltage which does not exceed ±1 V reduces by 66% compared to the traditional control scheme with ±3 V fluctuation.

Figure 5 shows the instantaneous active and reactive power flow in power cell. The instantaneous input active power p_{in} is equal to the load power of p_L. The instantaneous input reactive power q_{in} is close to zero. The instantaneous input active power p_{out} and reactive power q_{out} contain a DC component, besides, some oscillating components at 30 Hz, 40 Hz, 70 Hz, 100Hz, 140Hz, 170Hz, and 240Hz. The RMS of active power components and reactive power components are shown in Fig. 6. These results are consistent with (12) and (14).

Figure 7 shows the overall A phase input current and the currents of the power cell A1, B1, and C1 when the motor is running in 35 Hz. These harmonics, such as 20 Hz and 120 Hz, are cancelled out by the combined operation of the cells.

5 EXPERIMENT RESULTS

The experiment platform of power cell has been set up by taking two 32-bit digital signal processors as central processing unit (CPU), and circuit parameters are the same with the simulation shown in Tab. 1. The dead time of PWM is set as 2 μs. When the motor is running in 35 Hz, experiment results of output current and estimated load current are shown in Fig. 8. The estimated load current is outputted by a 10-bit DA chip. It can be seen clearly that, whether amplitude or phase, the load current can be identified in real time.

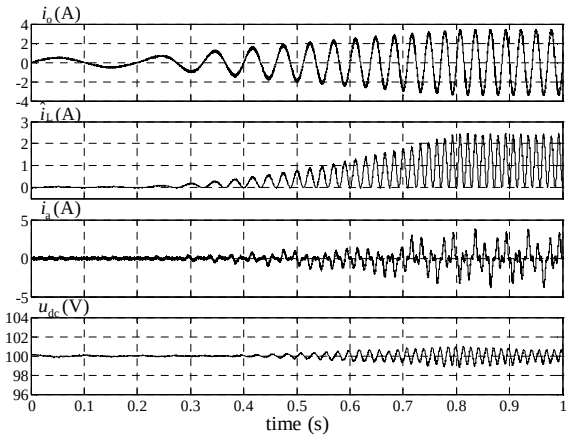

Fig. 4. Output current, estimated load current, input current, and DC link voltage when the motor speed increases

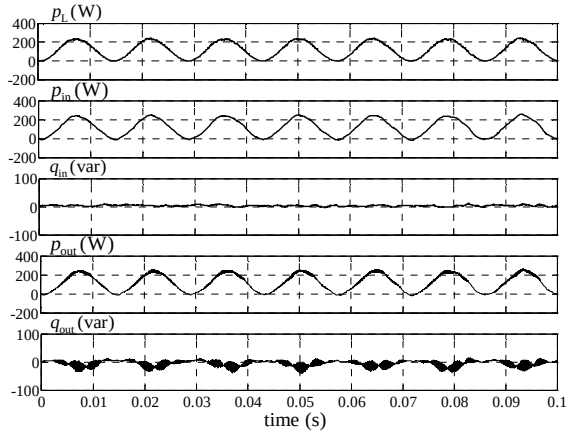

Fig. 5. Instantaneous active and reactive power

The experiment results of DC link voltage and input current without feed-forward compensation are shown in Fig. 9 (a). As can be seen, the fluctuation amplitude of DC link voltage is ±5 V. Fig. 9 (b) shows the DC link voltage and input current using the DAPC scheme with load current observer, the fluctuation amplitude is ±3 V. Fig. 9 (a) and (b) show that, the DAPC scheme with load current observer can significantly reduce the voltage fluctuation and increase the anti-disturbance of the system.

Although, theoretically it is possible to eliminate the fluctuation of DC link voltage, there are three limitations to obtain this result. First, the identified load current lags the

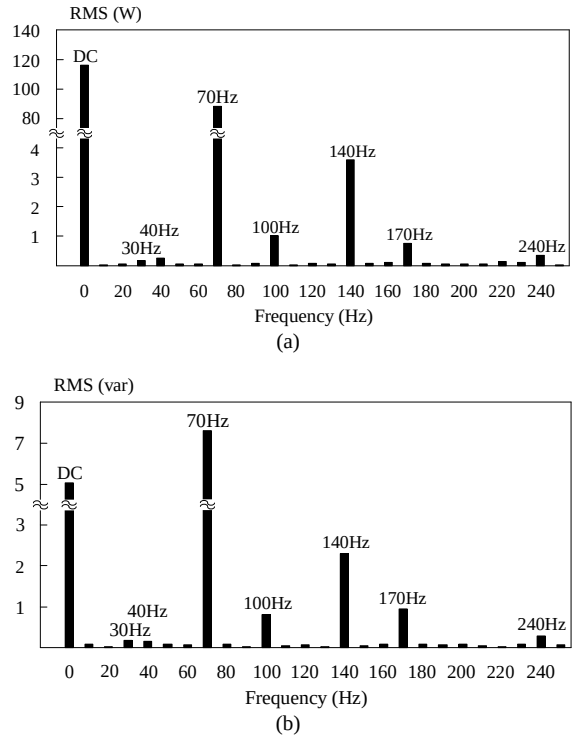

Fig. 6. The RMS of p_{out} and q_{out}: (a) active power components, (b) reactive power components

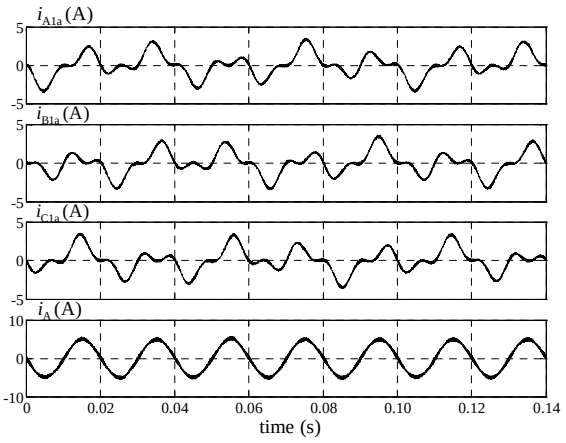

Fig. 7. A phase input currents when the motor is running in 35 Hz

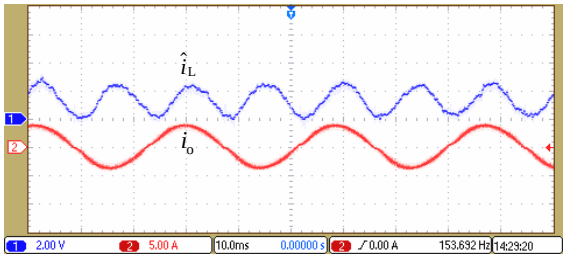

Fig. 8. Output current and estimated load current

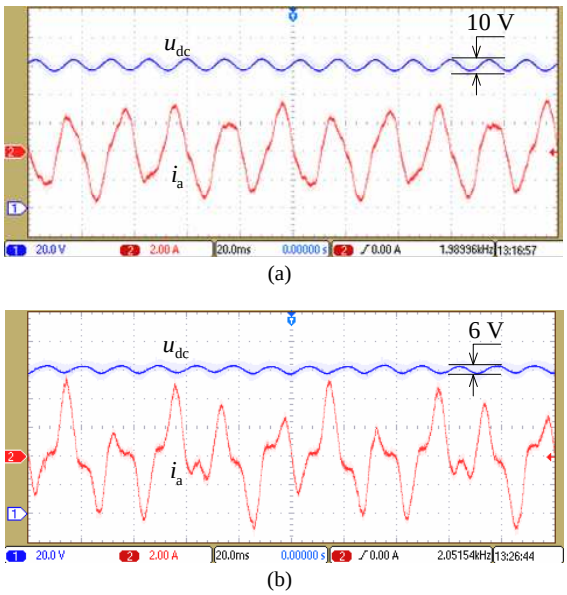

Fig. 9. DC link voltage and input current: (a) without feed-forward compensation, (b) with direct active power control scheme

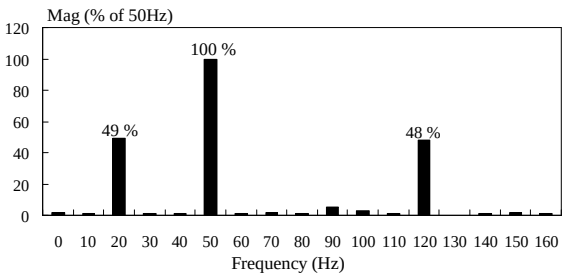

Fig. 10. FFT analysis of input current

actual current for a sampling period. Secondly, the current controller has limited bandwidth, and the dynamic slower than the reference change. Finally, sampling errors affect the identified results of load current and reduce the stability margin of the system. Thus, the input current does not follow fast enough the reference change, however, the fluctuation of DC link voltage is reduced to 60% of the original without additional equipments.

FFT analysis of the input current is shown in Fig. 10. As expected, the input current contains the harmonics at frequencies 20 Hz and 120 Hz. The frequency and amplitude of input harmonics changes as the load change which

are due to the proposed control scheme.

6 CONCLUSION

This paper presents the DAPC scheme for regenerative cascade inverter with reduced AC power in the DC Link. The DAPC scheme using the instantaneous *abc* theory in stationary three phase frame can control the instantaneous active power of the power cell under unbalanced equivalent filter inductances. Moreover, a load current full order observer is established to avoid the inconvenient of the current sensor installation. The experiment and simulation results prove the effectiveness of the proposed scheme.

As the load current has a relationship with the motor electrical angular frequency, to identify the real-time amplitude and phase of the load current, accurate observation model will be established in further study. Meanwhile, the time-delay compensation for the current controller will be studied to further reduce the voltage fluctuation in DC link.

REFERENCES

[1] M. Malinowski, K. Gopakumar, J. Rodriguez, and M. A. Perez, "A survey on cascaded multilevel inverters," *IEEE Transactions on Industrial Electronics*, vol. 57, no. 7, pp. 2197–2206, 2010.

[2] L. Xu, Y. Han, C. Chen, J. Pan, G. Yao, and L. Zhou, "Modeling, control and experimental investigation of a novel DSTATCOM based on cascaded H-bridge multilevel inverter," *Automatika -Journal for Control, Measurement, Electronics, Computing and Communications*, vol. 51, no. 1, pp. 41–54, 2010.

[3] I. Soares de Freitas, C. B. Jacobina, and E. C. dos Santos, "Single-phase to single-phase full-bridge converter operating with reduced ac power in the dc-link capacitor," *IEEE Transactions on Power Electronics*, vol. 25, no. 2, pp. 272–279, 2010.

[4] P. Lezana, J. Rodriguez, A. Marcelo, et al., "Input current harmonics in a regenerative multicell inverter with single-phase PWM rectifiers," *IEEE Transactions on Industrial Electronics*, vol. 56, no. 2 pp. 408–417, 2009.

[5] M. A. Perez, J. Espinoza, J. Rodriguez, and P. Lezana, "Regenerative medium-voltage AC drive based on a multicell arrangement with reduced energy storage requirements," *IEEE Transactions on Industrial Electronics*, vol. 52, no. 2, pp. 171–180, 2005.

[6] M. Mariusz, J. Marek, and P. K. Marian, "Simple direct power control of three-phase PWM rectifier using space-vector modulation (DPC-SVM)," *IEEE Transactions on Industrial Electronics*, vol. 51, no. 2, pp. 447–454, 2004.

[7] C. Jong-Woo and S. Seung-Ki, "Fast current controller in three- phase AC/DC boost converter using d-q axis crosscoupling," *IEEE Transactions on Power Electronics*, vol. 13, no. 1, pp. 179– 185, 1998.

[8] H. Akagi, Y. Kanazawa, and A. Nabae, "Instantaneous reactive power compensators comprising switching devices without energy storage components," *IEEE Transactions on Industry Applications*, vol. IA-20, no. 3, pp. 625–630, 1984.

[9] H. Namho, J. Jinhwan, and N. Kwanghee, "A fast dynamic DC-link power-balancing scheme for a PWM converter-inverter system," *IEEE Transactions on Industrial Electronics*, vol. 48, no. 4, pp. 794–803, 2001.

[10] J. Jinhwan, L. Sunkyoung, and N. Kwanghee, "A feedback linearizing control scheme for a PWM converter-inverter having a very small DC-link capacitor," *IEEE Transactions on Industry Applications*, vol. 35, no. 5, pp. 1124–1131, 1999.

[11] G. Bon-Gwan and placeN. Kwanghee, "A DC-link capacitor minimization method through direct capacitor current control," *IEEE Transactions on Industry Applications*, vol. 42, no. 2, pp. 573– 581, 2006.

[12] Y. Suh and T. A. Lipo, "Modeling and analysis of instantaneous active and reactive power for PWM AC/DC converter under generalized unbalanced network," *IEEE Transactions on Power Delivery*, vol. 21, no. 3, pp. 1530–1540, 2006.

[13] J. Hu and Y. He, "Modeling and control of grid-connected voltage-sourced converters under generalized unbalanced operation conditions," *IEEE Transactions on Energy Conversion*, vol. 23, no. 3, pp. 903–913, 2008.

[14] T. Furuhashi, S. Okuma, and Y. Uchukawa, "A study on the theory of instantaneous reactive power," *IEEE Transactions on Industrial Electronics*, vol. 37, no. 1, pp. 86–90, 1990.

[15] G. Rajesh and G. Narayanan, "Generalized feedforward control of single-phase PWM rectifiers using disturbance observers," *IEEE Transactions on Industrial Electronics*, vol. 54, no. 2, pp. 984–993, 2007.

[16] T. M. Jahns, T. A. Lipo, and V. Blasko, "New control method including state observer of voltage unbalance for grid voltage- source converters," *IEEE*

Transactions on Industrial Electronics, vol. 57, no. 6, pp. 2054–2065, 2010.

[17] L. Harnefors, M. Bongiorno, and S. Lundberg, "Input-admittance calculation and shaping for controlled voltage- source converters," *IEEE Transactions on Industrial Electronics*, vol. 54, no. 6, pp. 3323–3334, 2007.

[18] A. G. Yepes, F. D. Freijedo, O. Lopez, and J. Doval-Gandoy, "Analysis and design of resonant current controllers for voltage-source converters by means of nyquist diagrams and sensitivity function," *IEEE Transactions on Industrial Electronics*, vol. 58, no. 11, pp. 5231–5250, 2011.

[19] A.G. Yepes, F.D. Freijedo, and J. Doval-Gandoy, "Effects of discretization methods on the performance of resonant controllers," *IEEE Transactions on Power Electronics*, vol. 25, no. 7, pp. 1692–1712, 2010.

[20] L. Harnefors, "Implementation of resonant controllers and filters in fixed-point arithmetic," *IEEE Transactions on Industrial Electronics*, vol. 56, no. 4, pp. 1273–1281, 2009.

Changqing Qiu received the B.Sc. degree from Lanzhou University of Technology, China, in 2006 and M.Sc. degree from Wuhan University of Technology, China, in 2009. He is currently working toward the Ph.D. degree in State Key Laboratory of Advanced Electromagnetic Engineering and Technology of Huazhong University of Science and Technology (HUST), China. His main research interests include control of AC/DC/AC converters and electrical drives.

Shenghua Huang received a Ph.D. degree from HUST, China, in 1991, and is presently a professor at HUST. He has worked on new type of electrical machine theory and its control, power electronics and its applications in industry and power system. He is a member of China Electrotechnical Society.

Ende Wang received the B.Sc. degree from HUST, China, in 2008, and is currently working toward the Ph.D. degree at HUST. He has worked on new type of electrical machine and its control.

AUTHORS' ADDRESSES

Changqing Qiu, M.Sc.
Prof. Shenghua Huang, Ph.D.
Ende Wang, B.Sc.
College of Electrical and Electronic Engineering,
Huazhong University of Science and Technology,
Luoyu Load, 1037#, 430074, Wuhan, Hubei, P.R. China,
email: qiuchangqing@hust.edu.cn,
huangsh@163.com,wangende3321@163.com

Received: 2013-04-11
Accepted: 2013-09-02